BJES Basrah Journal for Engineering Sciences

Basrah Journal for Engineering Sciences, Vol. 22, No. 1, (2022), 58-68

Original Article

Journal homepage: www.bjes.edu.iq
ISSN (Online): 23118385, ISSN (Print): 18146120

OPEN ACCESS

Effect of Fiber Orientation Angle on Stress Intensity Factor of Composite Plate Using Extended Finite Element Method (XFEM)

Maha Sabah Kahyoosh [1,*], Rafil Mahmood Laftah [2], Ameen Ahmed Nassar [3]

[1,2,3] *Department of Mechanical Engineering, College of Engineering, University of Basrah, Basrah, Iraq*
E-mail addresses: maha94sabah@gmail.com , rafil.laftah@uobasrah.edu.iq , ameen.nassar@uobasrah.edu.iq
Received: 10 January 2022; Accepted: 8 March 2022; Published: 24 April 2022

Abstract

This paper presents the effect of fiber orientation angle on the stress intensity factor SIF for carbon epoxy composite plates with single-edge, center, and inclined cracks of varying lengths under tensile load. The stress intensity factor and shape factor were calculated individually for each case, with nine different fiber orientation angles computed using the extended finite element method XFEM concepts. It is found the stress intensity factor increases with increasing crack lengths while the shape factor decreases. In the case of single edge cracks, the SIF increases in the average value reached (173 %) for composite plates with different fiber orientation angles, while in the case of the center crack, the average value of SIF reaches (81 %). It was observed in this study that the increases in stress intensity factor and the decreases in the shape factor with different crack lengths were more stable in the composite plate with a fiber orientation angle of 75°. The higher values of SIF at an angle of 75° are because of the high probability of fiber slippage at 75° due to induced shear stresses in addition to the tensile stresses at the fiber-matrix interface. As a result, the crack tip has a high-stress intensity factor.

Keywords: Crack, Composite plate, Stress intensity factor, Shape factor, ABAQUS.

© 2022 The Authors. Published by the University of Basrah. Open-access article.
http://dx.doi.org/10.33971/bjes.22.1.7

1. Introduction

Composite materials are produced by combining two or more materials to create a new material with improved properties in comparison with each component. In this sense, reinforced concrete, as a blend of stone, sand, cement and steel, and wood consist of cellulose and lignin can be considered as a special type of composites. However, two main components are formed in the conventional forms of composites: fiber and matrix. Fibers are desired to reign a number of specifications, such as high elasticity modulus and ultimate strength and maintain their geometrical and mechanical properties during production and handling. The matrix must be chemically and thermally consistent with the fiber over a long time and should connect the fibers in one place, protect their surfaces and efficiently transfer stress to the fibers [1].

Composites' layered, orthotropic, sometimes inhomogeneous, and multi-material properties allow for the occurrence of various failure modes under varying loading conditions. However, the failure modes of composite plies can be divided into four categories: fiber failure, ply delamination, matrix cracking, and fiber/matrix deboning. These failure modes, or any combination of them, reduce and may eventually eliminate the composite action [1].

In composite laminates, fracture crack propagation takes place through any of the three modes or through a combination of the three modes. Mode I fracture (opening mode) represents the crack propagation under normal in plane loading where the crack is positioned perpendicular to the applied load. Mode II fracture (sliding mode) represents crack propagation due to shear type failure where the load applied is transverse to crack length. Mode III fracture (Tearing mode) represents crack propagation due to tear type failure where the load applied is parallel to the crack length. Mode I usually play a dominate role in engineering application and considered to be the most dangerous [2].

Dimitri and Fantuzzi (2017) [3] investigated the application of the level set method combined with the numerically extended finite element method (XFEM) to predict and calculate the direction of fracture propagation within the specimen stress intensity factor for different loading conditions under the cracked plate. The main results show that the SIF obtained from the XFEM method is in good agreement with accurate predictions in the literature, demonstrating the potential and efficiency of the XFEM method on singularity-driven fracture problems, even assuming limited mesh refinement near the crack tip. Gebru et al. [4] used a single edge notched composite laminate crack plate of carbon/epoxy orthotropic laminate to study the effect of fiber orientation angle on fracture toughness and determine the mode I stress intensity factor for the specimen by using analytical and finite element methods. The main results appear to show that the results of numerical methods are very close when numerical results are compared with finite method approaches, and the influence of the variation of fiber reinforcement angle on fracture toughness decreases with increasing fiber orientation angle Θ. In another study, Goli and Kazemi [5] evaluated the stress intensity factors for transversely isotropic functionally graded material FGMs by using the extended finite element method XFEM and the interaction integral method. The stress intensity factors for the different crack lengths and various material properties variations have been gained by this coupled

Copyright © 2022 the Authors. This is an open-access article distributed under the creative commons attribution License 4.0, which permits unrestricted use, distribution, and reproduction in any medium provided the original work is properly cited.

system of interaction integral and XFEM, which shows the efficiency of the presented framework. Benzaama et al. (2017) [6] used the XFEM method to determine the failure load for a unidirectional CFRP rectangular composite plate with a central elliptical, circular, and lateral V notch cutout under uniform uniaxial tensile loading. The results showed the notch weakens the structure and causes a reduction in the stiffness of the structure. Ultimate failure load magnitudes are decreased by increasing the notch size and can be increased by the appropriate between the type of modification and the shape of the notch in the case of the circular and elliptical notch. The crack and its propagation depend directly on the orientation of the fibers around the notch. Abdullah et al. [7] used the Extended Finite Element Method (XFEM) for modeling transversal cracks and delamination of carbon fiber composites, presenting the size effect of the composite due to the increment in composite thickness. The results showed good agreement between the experimental and analytical data of each specimen modeled based on the size of the carbon fiber composite volume.

The (ABAQUS) software uses the principles of the Extended Finite Element Method (XFEM) to calculate the values of the SIF. The purpose of XFEM was to calculate SIF in composite plates with different fiber orientation angles. So, this requires finding SIF in the crack tip. This work aims to study the effects of various fiber orientation angles and crack lengths on the stress intensity factor and shape factor.

2. Extended finite element method (XFEM)

The XFEM is a numerical technique that extends the traditional FEM approach through the extension of the solution space to differential solutions discontinuous function equations. The extended finite element method has been developed in order to alleviate problems with located features which cannot be resolved efficiently through mesh refinement. The modeling of fractures in a material was one of the first applications. With this original implementation discontinuous basis functions for nodes belonging to elements intersected by a crack are added to standard polynomial basis functions, providing a basis that includes crack opening displacement. An important advantage of XFEM is that the finite element mesh need not be updated for a crack path to track in such problems. More general use of the method to address problems of singularity, material interfaces, regular meshing of microstructural features such as voids, and other problems where an appropriate set of basic functions can describe a localized feature. It has been shown that such an integration of the problem into the approximation space can improve convergence rate and accuracy significantly in certain cases Furthermore, using extended finite element methods to solve problems with discontinuities eliminates the need to mesh and remesh the discontinuity surfaces, reducing computational costs and projection errors associated with traditional finite element methods while limiting the discontinuities to mesh edges [8].

The XFEM has an essential concept that is enriching in the approximation domain. Therefore, it can propagate some features of the issue of interest in certain discontinuities like the cracks and interface regions. Although it is a local version of the PUFEM enrichment utilized exclusively in a clear local domain, it has been highly reliant on the evolution of external enrichments for crack modeling by several meshless like (EFG) and (Hp-clouds). The main approximations of the XFEM developed for modeling the tough discontinuities in fracture mechanics problems. That later extended to include the weak discontinuity and interface issues [9].

The function of enrichment approximation $u(x)$ is presented in Eq. (1).

$$u^h(x) = u^{FE} + u^{enr} = \sum_{j=1}^{n} N_j(x)\, u_j + \sum_{k=1}^{m} N_k(x)\, \psi(x)\, a_k \qquad (1)$$

The $N_i(x)$ refer to the usual nodal shape functions, u is the vector of uniform degrees of nodal freedom in the FEM, a_k is the additional set of degrees of freedom to the classical *FE* model and $\Psi(x)$ is the function of discontinuous enrichment [10].

3. The stress intensity factor

The stress intensity factor for fracture mechanisms was used to determine stress intensity factor at the crack tip, especially because residual stresses were loaded remotely. The (SIF) is a theoretical value commonly applied to a homogeneous and linear elastic fracture mechanics (LEFM) material and is advantageous for providing criteria of the failure for fragile materials. The determination of the SIF can also be possible with its definition of the stress field and stress components need to be calculated as to which (K_I) is the result of extrapolation to the tip of a crack. This calculation is not exactly true to the definition of stress intensity factor (K_I) due to the stresses which are evaluated at the integration points and the tip of the crack is positioned within an element node. How the interpolation has to be done to achieve the best outcomes must constantly be examined [11].

Stress field and displacement which close to the tip of the crack have been considered as of important parameters to investigate the (SIF) values in linear elastic fracture mechanics via FE analysis, by using these parameters to predict the propagations of the crack and the failures under specific load conditions. Various (K_I) values calculation methods, for example, "virtual crack extension method", *J*-integer, and displacement correlation methods have been used. The SIF can be categorized as: "direct approach" and the "energy approach". The direct approach relates the SIF with the results of the FE method, while the second approach depends on the calculation value of the energy release rate *G* [2]. The stress at crack tip is shown at Fig. 1.

The function of the stress distribution near the tip of the crack [12] is given by:

$$\sigma_{xx} = \frac{K_I}{\sqrt{2\pi r}} \cos\frac{\theta}{2}\left(1 - \sin\frac{\theta}{2}\sin\frac{3\theta}{2}\right) \qquad (2)$$

$$\sigma_{yy} = \frac{K_I}{\sqrt{2\pi r}} \cos\frac{\theta}{2}\left(1 + \sin\frac{\theta}{2}\sin\frac{3\theta}{2}\right) \qquad (3)$$

Where, (r) is refers to the range from the crack tip, and (θ) is refers to the orientation. When the stress distribution in crack plane, the orientation parameter (θ) becomes zero and Eq. (2) and (3) will be reduced to Eq. (4) and (5):

$$\sigma_{xx} = \frac{K_I}{\sqrt{2\pi r}} \quad (4)$$

$$\sigma_{yy} = \frac{K_I}{\sqrt{2\pi r}} \quad (5)$$

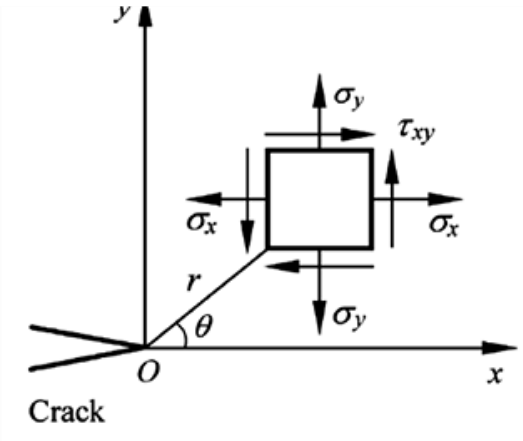

Fig. 1 Stress element at the crack tip.

4. Numerical simulation

4.1. Properties and Dimensions of the Plate

Composite plates used in this study are carbon epoxy with properties and dimensions show in Table 1 and 2 below. The composite plate has been subjected to various crack length, position, and different fiber orientation angles. The geometry of composite plate is shown in Fig. 2. We create composite lamina with 5 plies with same angles of fibers for each specimen.

Table 1. dimensions of the composite plates.

Material	Dimensions		
T700/8911 Composite laminates	Length	Width	Thickness
	240 mm	120 mm	5 mm

Table 2. properties of the composite plates [13].

Parameter	Properties	Unit
E_1	135	GPa
E_2	11.41	GPa
E_3	11.41	GPa
v_{12}	0.33	-
v_{13}	0.33	-
v_{23}	0.49	-
G_{12}	7.92	GPa
G_{13}	3.792	GPa
G_{23}	7.92	GPa
Max. principal stress X_T	2600	MPa
Fracture Energy G_{IC}	0.252	N/mm

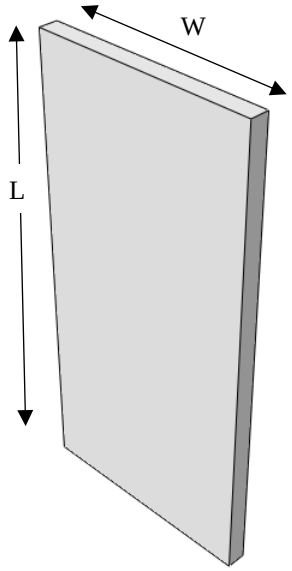

Fig. 2 the geometry of composite plate.

The analytical solution of stress intensity factor in isotropic plate including a central crack maybe found using equations (6), (7) and (8) [14].

$$K_I = Y\sigma\sqrt{\pi a} \quad (6)$$

$$Y = 1 + 0.256\left(\frac{a}{w}\right) - 1.152\left(\frac{a}{w}\right)^2 + 12.2\left(\frac{a}{w}\right)^3 \quad (7)$$

$$K_n = \sigma\sqrt{\pi a} \quad (8)$$

Where, (Y) is the shape factor.

The analytical and numerical values of SIF of the central cracked plate under uniform pressure 1 MPa are plotted against (a/w) for twelve crack length 10 to 120 mm with step 10 mm as shown in Fig. 3. This figure shows good agreement between the numerical and analytical values of SIF. It also could be noted from this figure that the value of Von Misses stress decrease when moving from the crack tip because the stress is concentrated at the tip of crack and less when moving from the tip of crack to the plate's boundaries.

The relation between crack length and shape factor $Y = K_I/K_n$ is shown in Fig. 4. The fringes stress distribution around crack tip for isotropic plate is shown in Fig. 5.

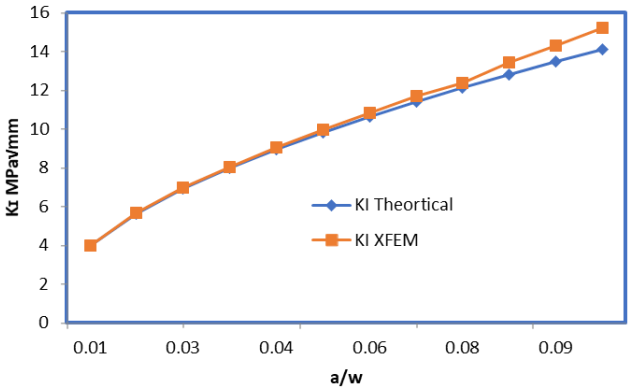

Fig. 3 effect of crack length on the stress intensity.

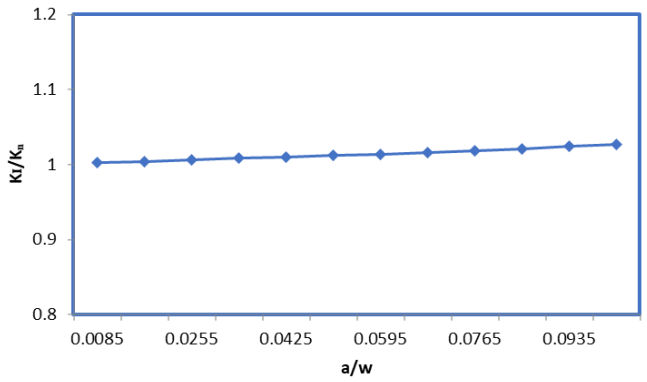

Fig. 4 effect of crack length on the shape factor.

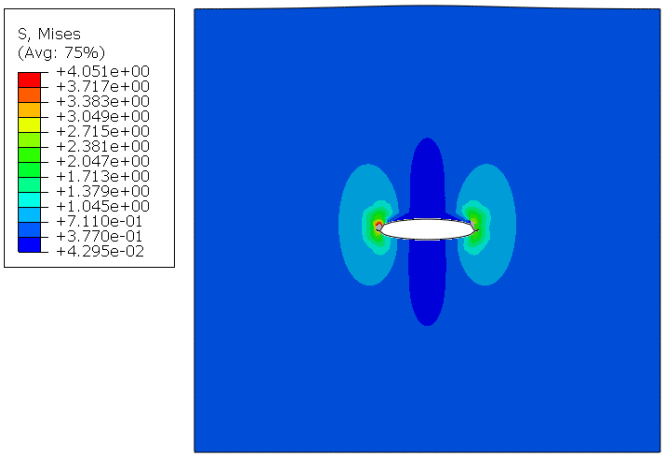

Fig. 5 stress distribution fringes.

4.2. the Calculation Technique of Stress Intensity Factor (K_I)

In this research, the calculation of SIF using the Meshless Local Petrov-Galerkin (MLPG) method had been achieved using a special technique, now is a profound definition about it. It is suggested to take a piece started exactly on the crack tip and extended straightly a head of the crack line (θ = 0) having length less than of (2 %) of the crack length ($s \leq 0.02a$), then, enough nodes will diffuse along this piece. To calculate SIF, an investigation of the stress field near/ahead of the crack tip will be done through calculating the stress at each node on the piece subsequently, plot on logarithmic scale these stresses against the effective radii (r_s) to the crack tip which have the singular value of stress. Then, a linear curve fitting on the got data will be achieved which absolutely represent the behavior of stress field nearly around/ahead of the crack tip, hence, its easily to get the singular stress at the crack tip ($r \approx 0$) from which it possible to use eq. (9) to estimate SIFs, see Fig. 6. Theoretically, it's known that the slop of the fitted line equals to (- 0.5) [15].

$$K_I = \sigma \sqrt{2\pi r} \tag{9}$$

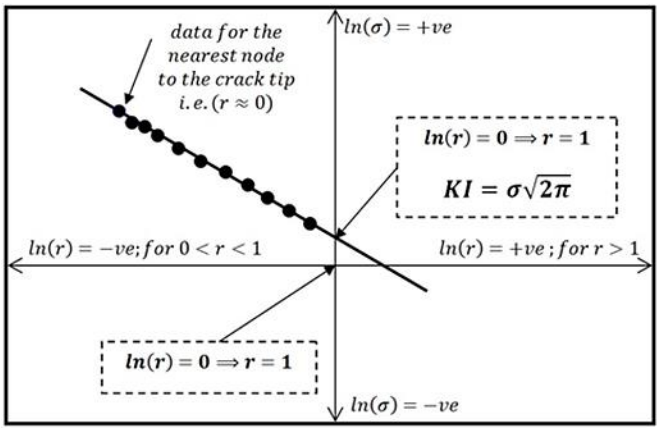

Fig. 6 SIFs calculation technique, where the fitted line represents the behavior of the singular stress field [16].

5. Effect of the fiber orientation angles (θ) of composite plate on the (SIF) K_I

Case 1: Composite Plate with Single Edge Crack

The values of the SIF against the ratio of (a/w) are shown in Fig. 8 for the composite plates with different fiber orientation angles (0°, 15°, 30°, 45°, 60°, 75°, 90°, 105°, 120°) with five different lengths of the crack (10 to 50 mm) by (10 mm) step. Fig. 9 shows the variation of the stress intensity factor around the crack tip for different fiber orientation angles. It is noticed that the stress intensity factor is maximum at an angle of 75 degrees, while the lowest value is at an angle of 15. Because the fibers are parallel to the crack front at an angle of 15, the number of discontinuous fibers at the crack front is very limited, and a large portion of the load is taken up by the matrix phase. As a result, the crack tip has a low-stress intensity factor distribution. There is a high probability of fiber slippage at 75 degrees due to induced shear stresses in addition to the tensile stresses at the fiber-matrix interface. As a result, the crack tip has a high-stress intensity factor. The number of continuous fibers sharing the far-field uniformly applied pressure intensity increases as the 75 degrees and above, resulting in a reduction in the stress intensity factor around the crack tip. Table 3 offers the SIF values for different fiber orientation angles. From this table observe how the stress intensity factor increases when the cracking length increases. Figure 7 represents the stress distribution around the crack tip in the composite plate with different angles of fiber for single edge cracks.

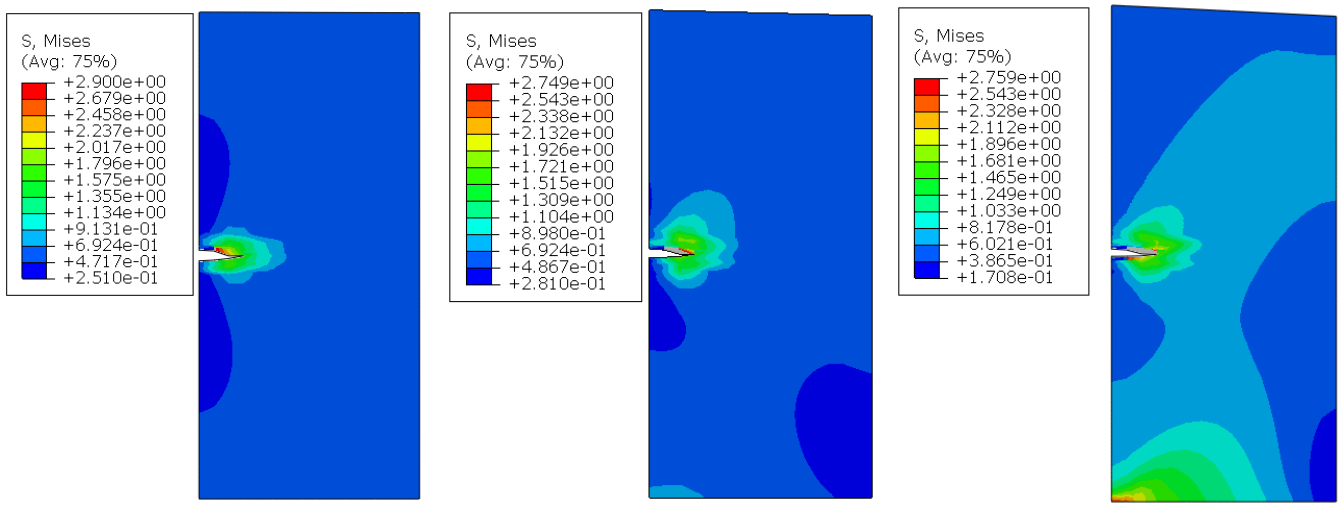

(a) angle of fiber 0° **(b)** angle of fiber 15° **(c)** angle of fiber 30°

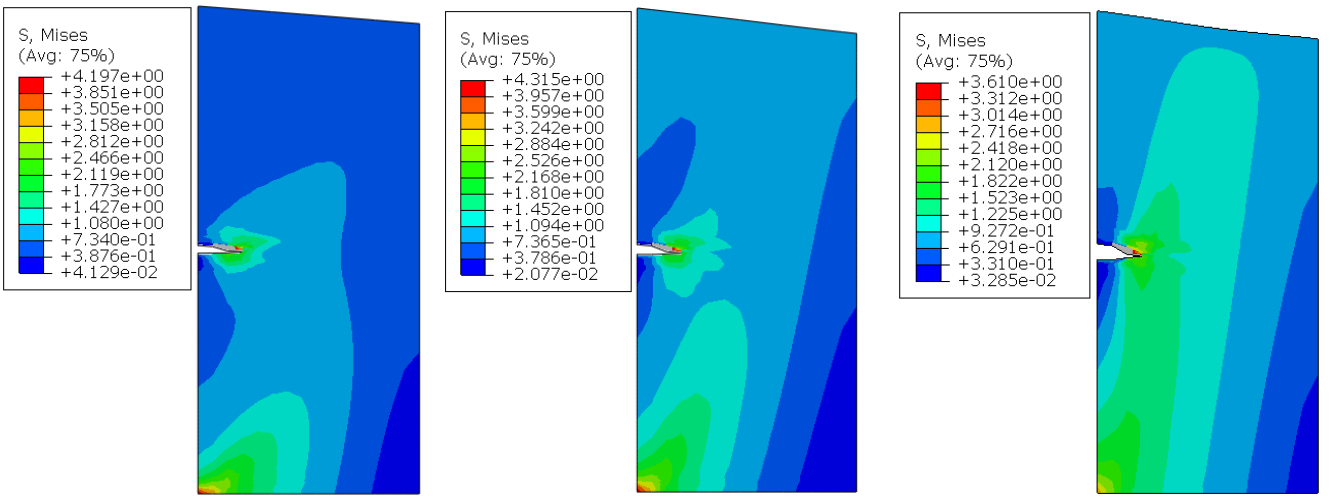

(d) angle of fiber 45° **(e)** angle of fiber 60° **(f)** angle of fiber 75°

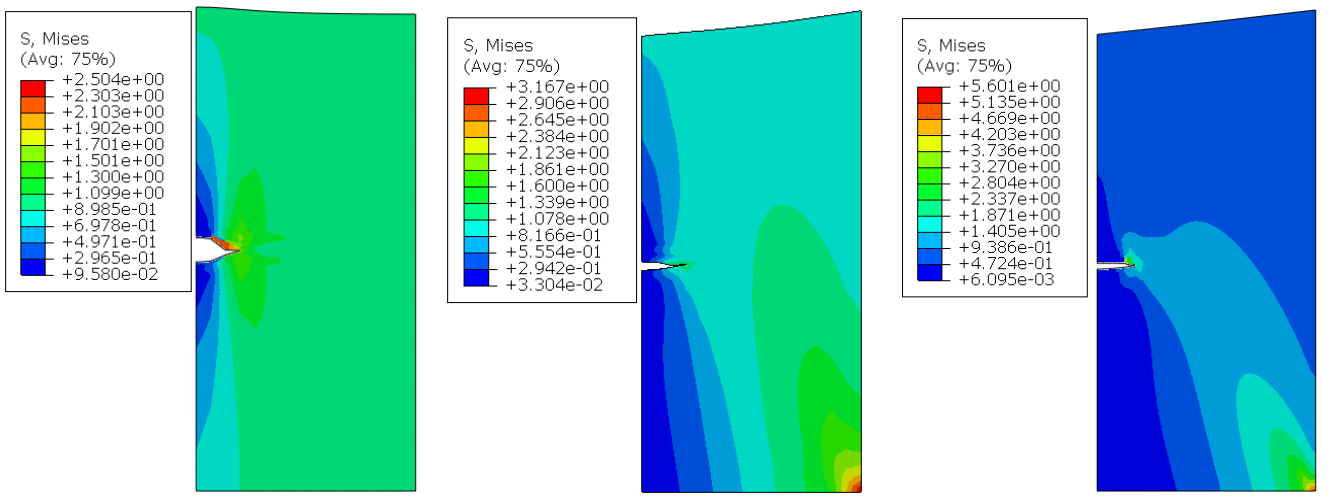

(h) angle of fiber 90° **(i)** angle of fiber 105° **(j)** angle of fiber 120°

Fig. 7 Stress distribution of composite plate with different angles of fiber for single edge cracks.

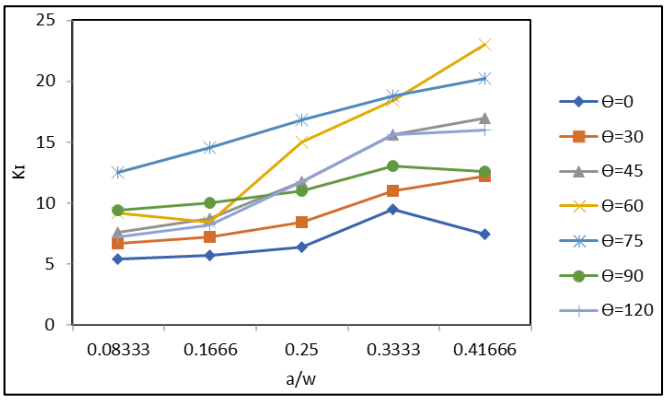

Fig. 8 Effect of crack length on the SIF in composited plates with different fiber orientation angles.

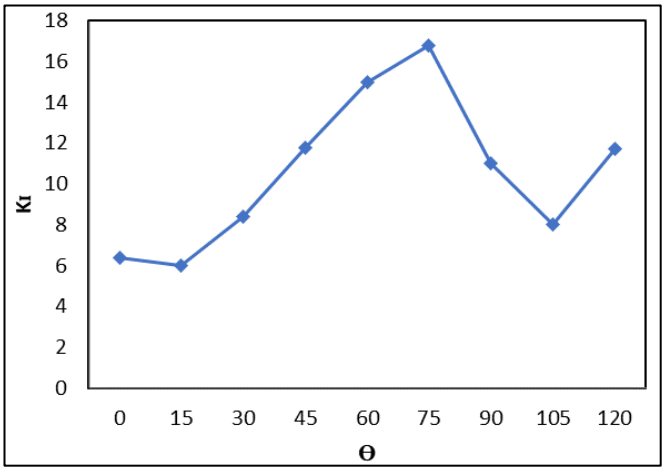

Fig. 9 SIF variations with fiber orientation angle θ for composite plate with single edge crack.

Table 3. the SIF values in composite plate with single edge crack.

a/w	SIF KI								
	Angle of Fiber θ								
	0°	15°	30°	45°	60°	75°	90°	105°	120°
0.08	5.4	5.4	6.7	7.6	9.2	12.5	9.4	4.6	7.2
0.16	5.7	5.6	7.2	8.7	11.6	14.5	10	5	8.2
0.25	6.4	6	8.4	11.75	15	16.8	11	8	11.7
0.33	9.5	6.8	11	15.6	18.4	18.8	13	9.4	15.6
0.41	7.4	6.9	12.2	16.95	23	20.2	12.6	15	16

The effect of the shape factor for different fiber orientation angles is shown in Fig. 10 and is presented in eq. (10) obtained from the DATA FIT program with a correlation factor (R^2 = 84.47 %). It is noted that, from the figures, the shape factor decreases with an increase in crack length, it is more stable when the angle of the fiber is at 75 degrees.

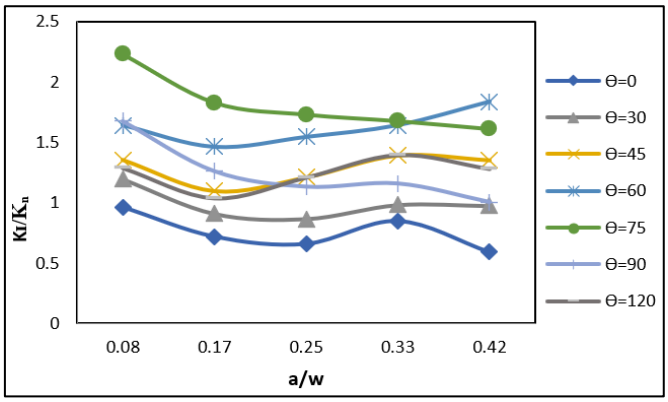

Fig. 10 Effect of crack length on shape factor Y for different fiber orientation angles of composite plate with single edge crack.

Were, $Y = K_I/K_n$

$$Y((a/w), \theta) = -2.3879 - 8.6981\ ln\ (a/w) - 8.40507\ ln\ (a/w)^2 - 3.3136\ ln\ (a/w)^3 - 0.45202\ ln\ (a/w)^4 + 1.309\ E\text{-}03\ (\theta) - 6.1546\ E\text{-}04\ (\theta)^2 + 4.0678\ E\text{-}05\ (\theta)^3 - 5.9262\ E\text{-}07\ (\theta)^4 + 2.4832\ E\text{-}09\ (\theta)^5 \quad (10)$$

This equation is available for the range: $0 \leq \theta \leq 120$

Case 2: Composite Plate with Center Crack

In this case, the composite plate has a center crack with length ($2a$) and different fiber orientation angles (0°, 15°, 30°, 45°, 60°, 75°, 90°, 105°, 120°). Figure 12 presents the relationship between the stress intensity factor in the first mode (K_I) and the ratio of crack length to plate width (a/w) for five various lengths of the crack (10 to 50 mm), taking into consideration a (10 mm) step for each increase in the length of the cracks. The variation of the stress intensity factor around the crack tip for different fiber orientation angles is shown in Fig. 13. It is observed that from this figure that the SIF is maximum at an angle of 75 degrees because there is a high probability of fiber slippage at 75 degrees due to induced shear stresses in addition to the tensile stresses at the fiber-matrix interface. As a result, the crack tip has a high-stress intensity factor. Table 4 offers the SIF values for different fiber orientation angles. From this table, observe how the stress intensity factor increases when the cracking length increases. Figure 11 represents the stress distribution around the crack tip in the composite plate with different angles of fiber for center cracks.

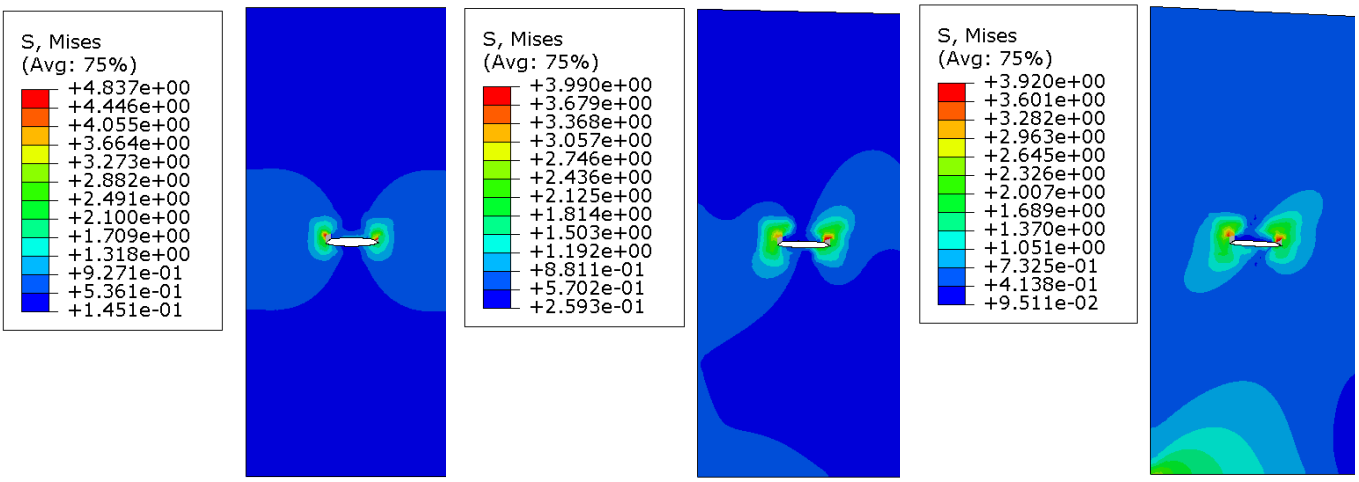

(a) angle of fiber 0° **(b)** angle of fiber 15° **(c)** angle of fiber 30°

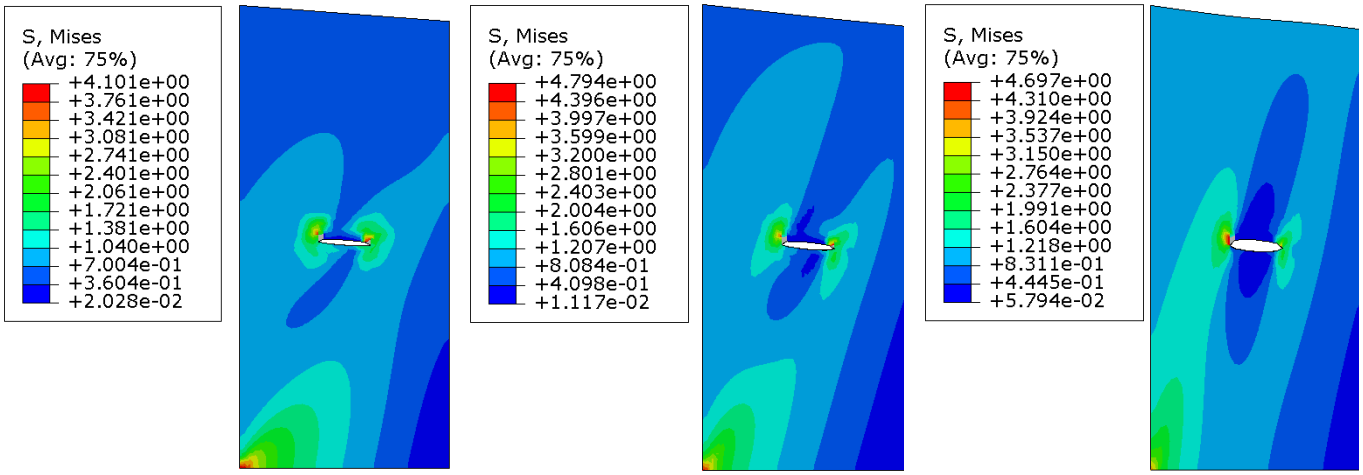

(d) angle of fiber 45° **(e)** angle of fiber 60° **(f)** angle of fiber 75°

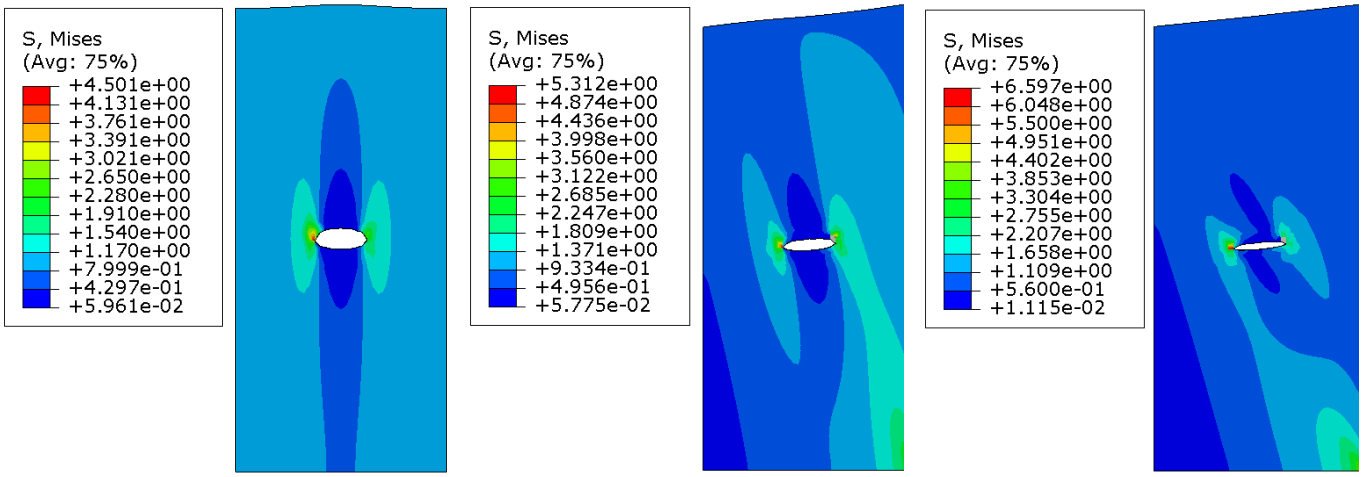

(h) angle of fiber 90° **(i)** angle of fiber 105° **(j)** angle of fiber 120°

Fig. 11 Stress distribution of composite plate with different angles of fiber for center cracks.

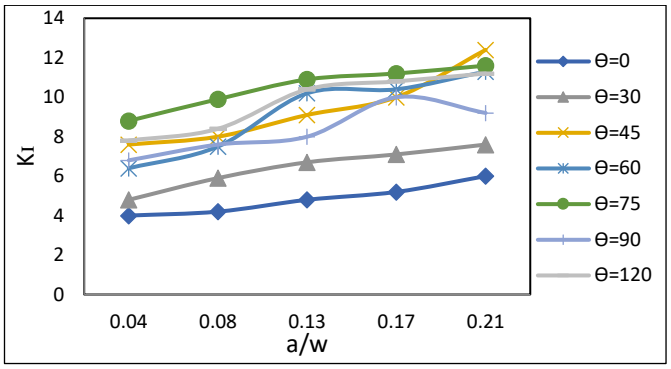

Fig. 12 Effect of crack length on the SIF in composited plates with different fiber orientation angles.

Table 4. the SIF values in composite plate with center crack.

a/w	SIF KI								
	Angle of Fiber θ								
	0°	15°	30°	45°	60°	75°	90°	105°	120°
0.04	4	4	4.8	7.6	6.4	8.8	6.8	7	7.8
0.08	4.2	4.16	5.9	8	7.5	9.9	7.6	7.6	8.4
0.12	4.8	4.6	6.7	9.1	10.2	10.9	8	10	10.4
0.16	5.2	4.9	7.1	10	10.4	11.2	10	11.6	10.8
0.20	6	5.2	7.6	12.4	11.3	11.6	9.2	12	11.2

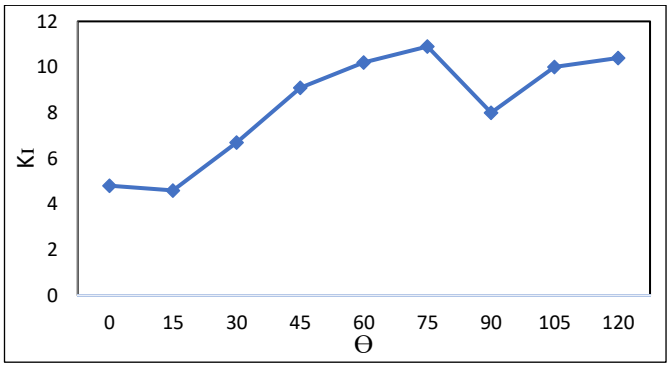

Fig. 13 SIF variations with fiber orientation angle (θ) for composite plate with center crack.

The effect of the shape factor for different fiber orientation angles (θ) is shown in Fig. 14 and is presented in eq. (11) that was obtained from the DATA FIT program with a correlation factor (R^2 = 90 %).

It is noted that, from figures, the shape factor decreases with an increase in crack length; it is more stable when the angle of the fiber is at 75 degrees.

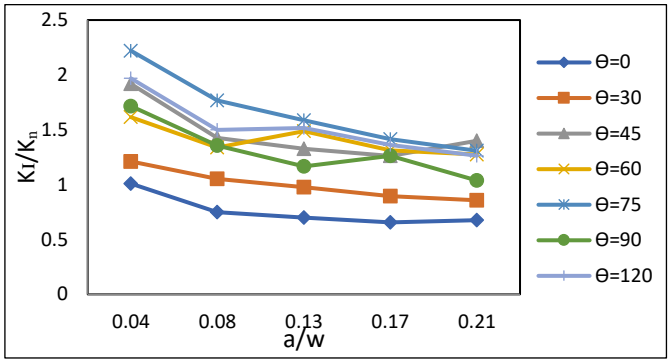

Fig. 14 Effect of crack length on shape factor *Y* for different fiber orientation angles of composite plate with center crack.

$$Y\,(a/w,\,\theta) = 241.922 - 13174.158\,(a/w) + 259178.259\,(a/w)^2 - 2347286.454\,(a/w)^3 + 9933628.008\,(a/w)^4 - 15884508.088\,(a/w)^5 - 3.3267\text{ E-}02\,(\theta) + 2.5972\text{ E-}03\,(\theta)^2 - 4.90118\text{ E-}05\,(\theta)^3 + 3.65889\text{ E-}07\,(\theta)^4 - 9.572101\text{ E-}10\,(\theta)^5 \quad (11)$$

This equation is available for the range: $0 \le \theta \le 120$

Case 3: Composite Plate with Inclined Edge Crack

An inclined edge crack in a composite plate under tensile loading was analyzed numerically depending on the XFEM concepts by using the program software ABAQUS. Fig. 15 represents the geometry, mesh, and boundary condition of the composite plate with an inclined edge crack. Figure 16 present the values of the stress intensity factor in mode I and mode II SIFs, respectively, K_I and K_{II}, which plot against the ratio of (a/w) for the composite plates with a crack angle (β) ranging from 15° to 75° measured counterclockwise from the horizontal axis and with different fiber orientation angles with five different lengths of the crack (10 to 50 mm) by (10 mm) step. It is noted from this figure that the values of the stress intensity factor K_I and K_{II} increase when the crack lengths increase for the same crack angle (β), and an increasing rate of K_I is very significant at small crack angles, while the rate of increase of K_{II} is low at high crack angles. Tables 5 and 6 offer the SIF values for modes I and II for different fiber orientation angles at the ratio of (a/w = 0.125) and with various crack angles (β).

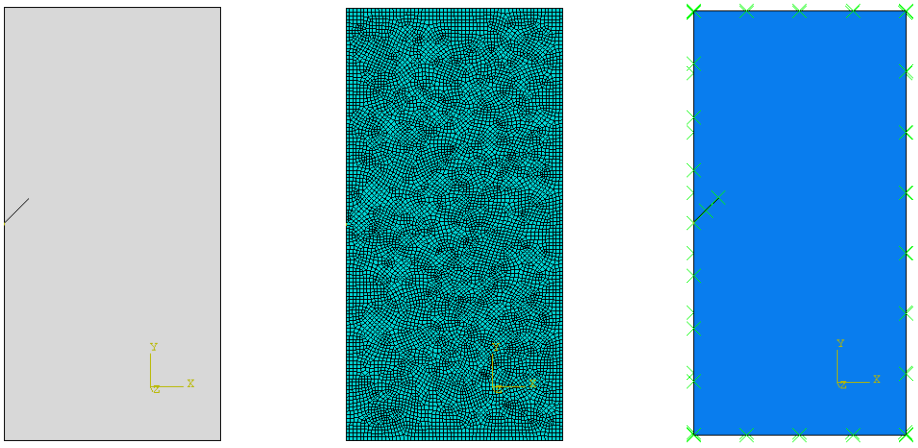

(a) plate with inclined edge crack. **(b)** mesh of plate. **(c)** B.C. of plate.

Fig. 15 inclined edge crack specimen.

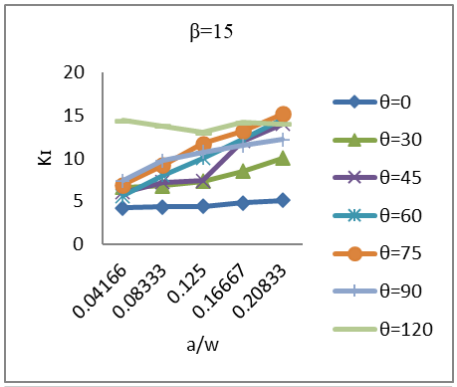
β=15
KI
a/w
θ=0
θ=30
θ=45
θ=60
θ=75
θ=90
θ=120

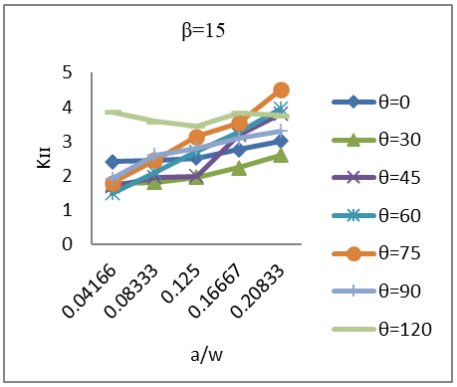
β=15
KII
a/w
θ=0
θ=30
θ=45
θ=60
θ=75
θ=90
θ=120

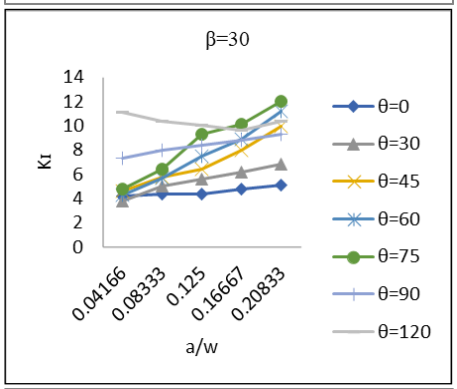
β=30
KI
a/w
θ=0
θ=30
θ=45
θ=60
θ=75
θ=90
θ=120

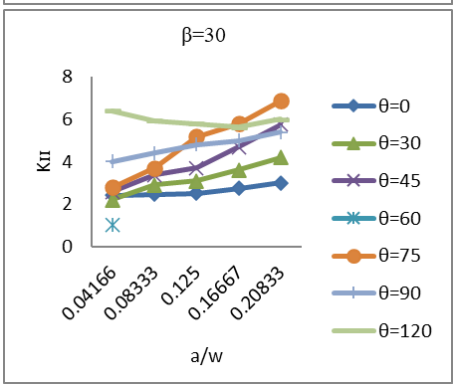
β=30
KII
a/w
θ=0
θ=30
θ=45
θ=60
θ=75
θ=90
θ=120

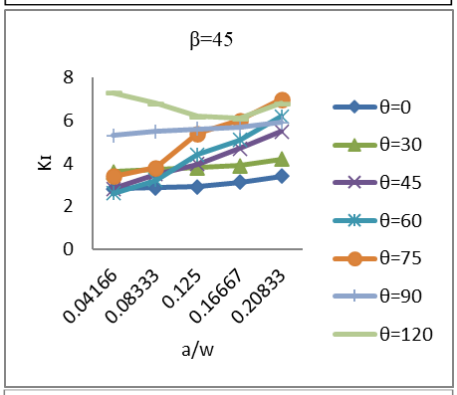
β=45
KI
a/w
θ=0
θ=30
θ=45
θ=60
θ=75
θ=90
θ=120

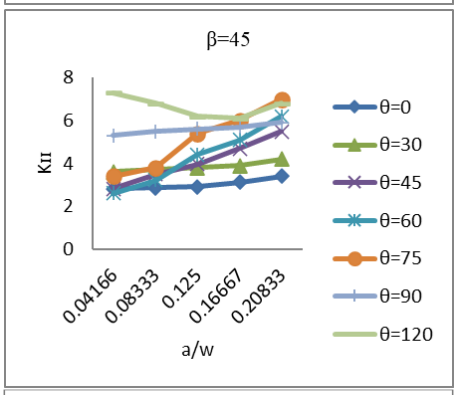
β=45
KII
a/w
θ=0
θ=30
θ=45
θ=60
θ=75
θ=90
θ=120

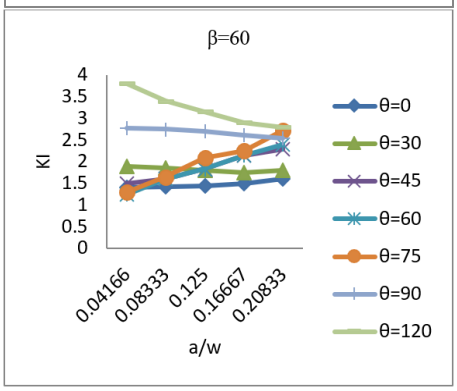
β=60
KI
a/w
θ=0
θ=30
θ=45
θ=60
θ=75
θ=90
θ=120

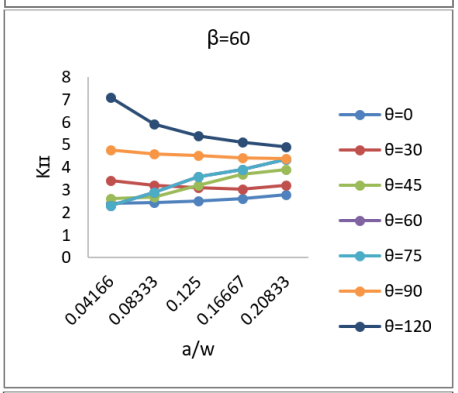
β=60
KII
a/w
θ=0
θ=30
θ=45
θ=60
θ=75
θ=90
θ=120

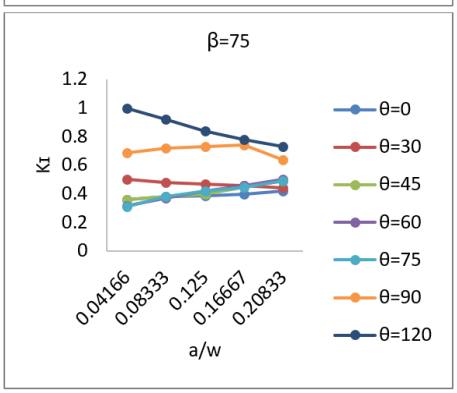
β=75
KI
a/w
θ=0
θ=30
θ=45
θ=60
θ=75
θ=90
θ=120

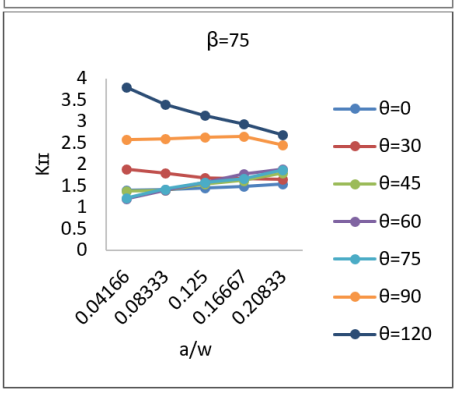
β=75
KII
a/w
θ=0
θ=30
θ=45
θ=60
θ=75
θ=90
θ=120

Fig. 16 effect of the length of crack on SIF mode I K_I and mode II K_{II} in inclined edge cracks for composite plates at different fiber orientation angles and with different crack angles (β).

Fig. 17 shows that as crack angle (β) increases, K_I decreases until it reaches a minimum value at β = 75° and a maximum value at β = 15°, for the same crack length, because of the anticipated reduction in the contribution of the force acting normal to the crack surface. Fig. 18 offers that K_{II} values increase from a minimum value at β = 15° to reach a maximum value at β = 45° followed by a decrease in K_{II} to reach minimum value at β = 75°.

Fig. 19 depicts the effect of different fiber orientation angles on the SIF for modes I and II. It is observed that when the fiber angle is 120° and the crack angle is 15°, K_I reaches its maximum value, whereas K_{II} reaches its high magnitude when the fiber orientation angle is 120° and the crack angle is 45°.

Table 5. the SIF mode I value in composite plate with inclined edge crack.

β	SIF K_I								
	Angle of Fiber θ								
	0°	15°	30°	45°	60°	75°	90°	105°	120°
15°	5.6	5.6	7.3	7.4	10	11.7	10.7	7	13
30°	4.4	4.4	5.58	6.4	7.5	9.3	8.4	5.4	10
45°	2.9	2.9	3.8	3.97	4.4	5.4	5.6	3.2	6.2
60°	1.45	1.45	1.8	1.83	1.83	2.1	2.7	1.3	3.15
75°	0.39	0.39	0.47	0.4	0.42	0.42	0.73	0.24	0.84

Table 6. the SIF mode II values in composite plate with inclined edge crack.

β	SIF K_{II}								
	Angle of Fiber θ								
	0°	15°	30°	45°	60°	75°	90°	105°	120°
15°	1.48	1.48	1.95	1.97	2.7	3.14	2.8	1.8	3.45
30°	2.5	2.5	3.1	3.7	4.2	5.18	4.8	3.08	5.8
45°	2.9	2.9	3.8	3.97	4.4	5.4	5.6	3.2	6.2
60°	2.5	2.5	3.1	3.2	3.2	3.6	4.53	2.3	5.4
75°	1.45	1.45	1.7	1.55	1.59	1.58	2.5	0.95	3.15

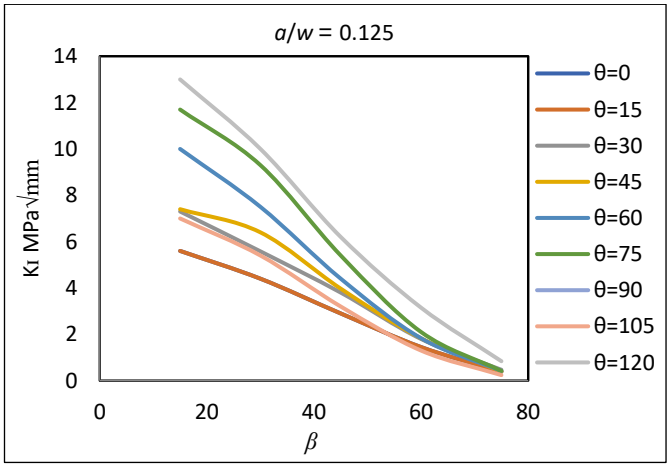

Fig. 17 effect of inclined angles on SIF mode I in slanted edge crack for composite plate.

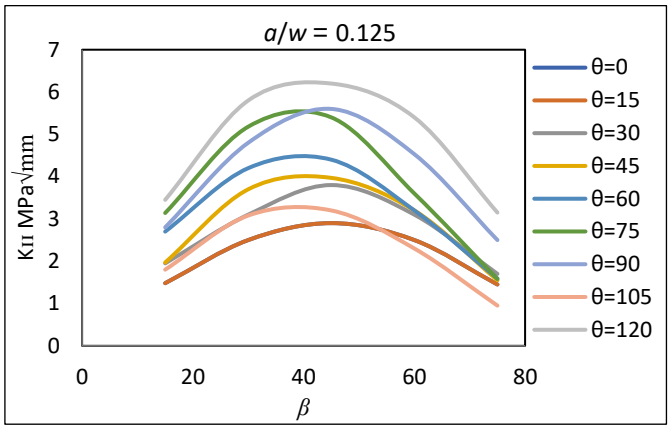

Fig. 18 effect of inclined angles on SIF mode II in slanted edge crack for composite plate.

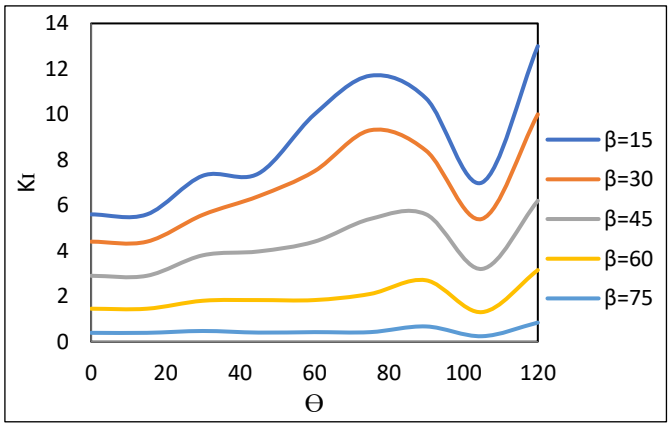

(a) K_I

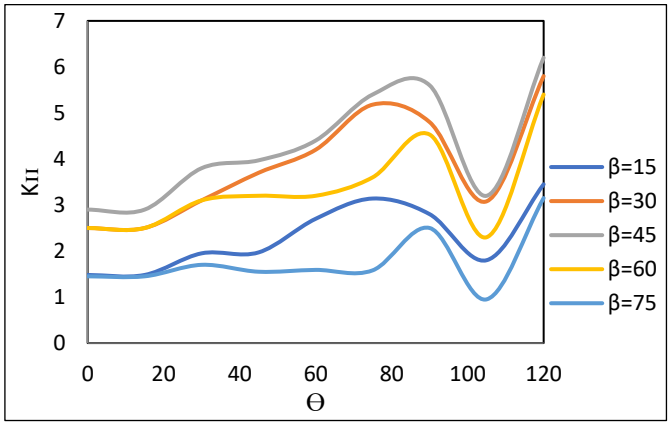

(b) K_{II}

Fig. 19 effect of different fiber orientation angles on the SIF in composited plates with different crack angles (β).

7. Conclusions

In this study, the values of the stress intensity factor (K_I) and shape factor (Y) are determined by using the extended finite element methods (XFEM) for carbon epoxy composite plates with different fiber orientation angles that are loaded with uniaxial tension. The obtained results led to the following conclusions:

1. In the case of single edge cracks, the increase in the average value of SIF reached 173 percent for composite plates with different fiber orientation angles, while in the case of the center crack, the average value of SIF reached (81 %).
2. For two cases, single edge crack and center crack in the carbon epoxy composite plate with different fiber orientation angles, the stress intensity factor increases with increased crack length up to its maximum value at an angle of 75 degrees because of the high probability of fiber slippage at 75 degrees due to induced shear stresses in addition to the tensile stresses at the fiber-matrix interface. As a result, the crack tip has a high-stress intensity factor.
3. Increases in stress intensity factor and shape factor for composite plates with edge and center cracks of varying lengths are more stable in plates with a fiber orientation angle of 75°.
4. In the case of an inclined edge crack composite plate, both model I and II stress intensity factors (SIF) increase with increasing crack length. However, the rate of increase in mode I SIF decreases with increasing the crack angle.
5. For the same crack length, mode II (SIF) increases with increasing crack angle to reach a maximum value at crack angle 45°, followed by a decrease in mode II (SIF). At fiber orientation angle 120, K_I and K_{II} reach their maximum values.

References

[1] Soheil Mohammadi, XFEM Fracture Analysis of Composites, John Wiley & Sons, Ltd., ISBN 978-1-119-97406-2, 2012.

[2] T. L. Anderson, Fracture Mechanics: Fundamental and Applications, Taylor & Francis Group, LLC, ISBN 978-1-4987-2813-3, 2017.

[3] R. Dimitri, N. Fantuzzi, Y. Li, and F. Tornabene, "Numerical computation of the crack development and SIF in composite materials with XFEM and SFEM", Composite Structures, Vol. 160, pp. 468-490, 2017. https://doi.org/10.1016/j.compstruct.2016.10.067

[4] E. Gebru, K. Jain "Effect of Fiber Orientation Angle on Stress Intensity Factor of Composite Laminated Crack Plate", International Journal for Research in Applied Science & Engineering Technology (IJRASET), Vol. 6, Issue 4, pp. 4700-4706, 2018. https://doi.org/10.22214/ijraset.2018.4772

[5] E. Goli and M. T. Kazemi, "XFEM Modeling of Fracture Mechanics in Transversely Isotropic FGMs via Interaction Integral Method", Procedia Materials Science, Vol. 3, pp. 1257-1262, 2014. https://doi.org/10.1016/j.mspro.2014.06.204

[6] A. Benzaama, M. Mokhtari, H. Benzaama, S. Gouasmi, and T. Tamine, "Using XFEM technique to predict the damage of unidirectional CFRP composite notched under tensile load", Advances in aircraft and spacecraft science, Vol. 5, Issue 1, pp. 129-139, 2018. https://doi.org/10.12989/aas.2018.5.1.129

[7] N. A. Abdullah, J. L. Curiel-Sosa, Z. A. Taylor, B. Tafazzolimoghaddam, J. L. M. Vicente, and C. Zhang, "Transversal crack and delamination of laminates using XFEM", Composite Structures, Vol. 173, pp. 78-85, 2017. https://doi.org/10.1016/j.compstruct.2017.04.011

[8] D. Datta, "Introduction to Extended Finite Element (XFEM) Method", e-print arXiv, Computational Physics, 2013. https://doi.org/10.48550/arXiv.1308.5208

[9] S. Jiang, Z. Ying, and Ch. Du, "The optimal XFEM approximation for fracture analysis the optimal XFEM approximation for fracture analysis", IOP Conference Series: Materials Science and Engineering, Vol. 10, pp. 1-9, 2010. https://doi.org/10.1088/1757-899X/10/1/012067

[10] H. I. Khalaf, "Crack Propagation in Plane Stress Problems by Using Experimental and Extended Finite Element Method," Ph.D. thesis, Mechanical Engineering Department, College of Engineering, University of Basrah, October 2015.

[11] A. O. Mashjel, R. M. Laftah, and H. I. Khalaf, "Study the effect of perforation type for plate with central crack on the stress intensity factor using the XFEM", Basrah Journal for Engineering Sciences, Vol. 21, No. 1, pp. 27-37, 2021. https://doi.org/10.33971/bjes.21.1.5

[12] R. M. Laftah, "Study of Stress Intensity Factor in Corrugated Plate Using Extended Finite Element Method (XFEM)", Engineering and Technology Journal, Vol. 34, No. 15, pp. 2982-2992, 2016.

[13] P. F. Liu, Y. H. Yang, Z. P. Gu, and J. Y. Zheng, "Finite Element Analysis of Progressive Failure and Strain Localization of Carbon Fiber/Epoxy Composite Laminates by ABAQUS", Applied Composite Materials, Vol. 22, pp. 711-731, 2015.https://doi.org/10.1007/s10443-014-9432-1

[14] S. Saad Nama, and R. M. Laftah, "Investigation of Stress Intensity Factor for Corrugated Plates with Different Profiles Using Extended Finite Element (XFEM)", Basrah Journal for Engineering Sciences, Vol. 18, No. 1, pp. 1-9, 2018. https://doi.org/10.33971/bjes.18.1.1

[15] L. S. Al-Ansari, H. N. Al-mahmud, and S. K. Al-raheem, "Calculating Stress Intensity Factor (Mode I) for Composite Plate with Central Crack", International Journal of Computer Applications, Vol. 75, No. 15, pp. 1-10, August 2013. https://doi.org/10.5120/13184-0671